Achieving and Validating the 1-centimeter Orbit: Jason-1 Precision Orbit Determination Using GPS, SLR, DORIS and Altimeter data

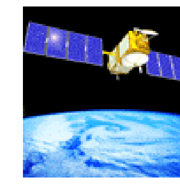

S.B. Luthcke[1], N.P. Zelensky[2], D.D. Rowlands[1], T.A. Williams[2], F.G. Lemoine[1]

[1] NASA Goddard Space Flight Center, Greenbelt Maryland, USA

[2] Raytheon ITSS, Upper Marlboro Maryland, USA

ABSTRACT

Jason-1, launched on December 7, 2001, is continuing the time series of centimeter level ocean topography observations as the follow-on to the highly successful TOPEX/POSEIDON (T/P) radar altimeter satellite. The precision orbit determination (POD) is a critical component to meeting the ocean topography goals of the mission. Jason-1 is no exception and a 1 cm radial orbit accuracy goal has been set. This represents a factor of two improvement over what is currently being achieved for T/P. The challenge to precision orbit determination (POD) is both achieving the 1 cm radial orbit accuracy and evaluating and validating the performance of the 1 cm orbit. Fortunately, Jason-1 POD can rely on four independent tracking data types including near continuous tracking data from the dual frequency codeless BlackJack GPS receiver. In addition, to the enhanced GPS receiver, Jason-1 carries significantly improved SLR and DORIS tracking systems along with the altimeter itself.

We demonstrate the 1 cm radial orbit accuracy goal is being achieved using GPS data in a reduced dynamic solution. It is also shown that adding SLR data to the GPS-based solutions improves the orbits even further. In order to assess the performance of these orbits it is necessary to process all of the available tracking data (GPS, SLR, DORIS and altimeter crossover differences) as either part of or independent of the orbit solutions. It was also necessary to compute orbit solutions using various combinations of the four available tracking data in order to independently assess the orbit performance. Towards this end, we have greatly improved orbits determined solely from SLR+DORIS data by applying the reduced dynamic solution strategy. In addition, we have computed reduced dynamic orbits based on SLR, DORIS and crossover data that are a significant improvement over the SLR and DORIS based dynamic solutions. These solutions provide the best performing orbits for independent validation of the GPS-based reduced dynamic orbits.

POD Overview and Details

Overview: ***In selecting orbit solution strategies, we sought to determine the best orbit and then characterize the orbit error. In order to properly characterize orbit error, it is important to compare two orbits of near equal performance determined from independent tracking. In this poster we summarize our analysis from five candidate orbit solution strategies that run the spectrum of data combination and parameterization: (1) SLR and DORIS dynamic (SLR+DORIS Dyn.), (2) SLR and DORIS reduced dynamic (SLR+DORIS RD), (3) SLR, DORIS and altimeter crossover reduced dynamic (SLR+DORIS+Xover RD), (4) GPS reduced dynamic (GPS RD), and (5) GPS and SLR reduced dynamic (GPS+SLR RD). The analysis uses data from cycles 8-24 as the test data set over which all solution strategies are compared. Further details can be found in Luthcke et al. 2003.***

Table 1 **POD Summary(1): Models, Data and Parameters**

Geophysical Models and Parameters	
Gravity / Tides	JGM3 [1], GGM01S [2] / GOT99.2 [3]
Atmospheric Density	MSIS-86 [4]
Station Coordinates	ITRF2000
Earth Orientation	IERS C 04
Planetary Ephemeris	DE403
Tracking Data	
GPS	• Double differenced, ionosphere-free combination of L1 and L2 carrier phase (DDLC). • ~33 IGS Stations (best performing / optimal distribution)
SLR / DORIS/ Altimeter Crossovers	DORIS "SAA" station data included; light editing of altimeter crossover data
Modeling	
Jason-1	• GSFC antenna LC Phase Correction (APC) map • *a priori* GPS antenna LC phase center offset in S/C Body Fixed (SBF): ○ (SBF X, Y, Z); (2.389, -0.218, -0.504) (m) • estimated SLR offset in SBF: ○ (SBF X, Y, Z); (1.158, 0.598, 0.6828) (m) • *a priori* DORIS offset in SBF: ○ (SBF X, Y, Z); (1.171, -0.598, 1.027) (m) • *a priori* center of mass offset in SBF: ○ (SBF X, Y, Z); (0.942, 0.000, 0.000) (m) • GPS antenna orientation unit vectors in SBF: ○ Boresite (SBF X, Y, Z); (0.498, -0.044, -0.866) ○ X Dipole (SBF X, Y, Z); (0.867, 0.025, 0.497) • SLR retro-reflector range correction: -0.049 m • s/c orientation: ○ telemetered quaternions (attitude model as needed) • s/c area and solar radiation pressure: pre-launch "Box-wing" model[5]
GPS Satellites	• IGS final/precise GPS ephemerides - Edited • IGS Block II, IIA, IIR phase center of mass offsets • New GPS satellite attitude (Bar-Sever, 1996)
GPS Stations	Antenna phase center
SLR/DORIS/GPS	Troposphere refraction
GPS	• Outlier editing / cycle slip detection and correction • Phase wind-up • GPS receiver pre-process clock correction for 2nd order effect

1 Tapley, B.D. M.M. Watkins, J.C. Ries, G.W. Davis, R.J. Eanes, S.R. Poole, H.J. Rim, B.E. Schutz, C.K. Shum, R.S. Nerem, F.J. Lerch, J.A. Marshall, S.M. Klosko, N.K. Pavlis and R.G. Williamson. 1996. The JGM-3 geopotential model. *Journal of Geophysical Research*. 101: 28029-28049.
2 Tapley, B., S. Bettadpur, M. Watkins and Ch. Reigber, "The Gravity Recovery and Climate Experiment; Mission Overview and Early Results," in preparation, 2003.
3 Ray, R.D. 1999. A global Ocean Tide Model From TOPEX/POSEIDON Altimetry: GOT99.2, NASA/TM-1999-209478, GSFC.
4 Hedin, A.E. 1988. The atmosphere model in the region 90 to 200km, *Adv. Space Res*. 8(5): 9-25.
5 CNES POD Team - http://calVAL.jason.oceanobs.com/html/calval_plan/poe/models_jason.html

Table 2 **POD Summary (2): Data Weighting, Estimated Parameters and Arc Length**

Data Weighting	
Data Sigma Weighting	SLR/DORIS Dynamic: 10 cm SLR; 20 mm/s DORIS SLR/DORIS Reduced Dynamic: 10 cm SLR; 10 mm/s DORIS SLR/DORIS/Crossover Reduced Dynamic: 10 cm SLR; 10 mm/s DORIS; 10 cm Crossover SLR/GPS Reduced Dynamic: 10 cm SLR; 10 cm GPS
Estimated Parameters	
Measurement Model	• GPS carrier phase ambiguity per pass • GPS troposphere scale factor every 60 min. / station • DORIS measurement bias and troposphere scale factor per pass
Force Model	• SLR/DORIS based solution Dynamic Parameterization: ○ State (pos. and vel.); C_D / 8 hr.; Alg and Crs 1-cpr accelerations / 24 hr. • SLR/DORIS based solution Reduced Dynamic Parameterization: ○ State (pos. and vel.); C_D / 24 hr.; Alg and Crs 1-cpr accelerations / 28 min; 45 min correlation time; 1.e-9 m/s^2 sigma • GPS based solution Reduced Dynamic Parameterization: ○ State (pos. and vel.); C_D / 30 hr.; Alg and Crs 1-cpr accelerations / 30 min; 60 min correlation time; 1.e-9 m/s^2 sigma • GPS/SLR based solution Reduced Dynamic Parameterization: ○ State (pos. and vel.); C_D / 30 hr.; Alg and Crs 1-cpr accelerations / 30 min; 60 min correlation time; 5.e-9 m/s^2 sigma
Arc Length / Details	
Short Arcs	GPS Orbit solutions computed in 30-hr. arcs with 6-hr. overlapping time periods. The arcs do not necessarily start on 0-hrs of a day, but are constructed such that 10 short arcs evenly cover a Jason-1 repeat cycle.
Long Arcs	A long arc covers a Jason-1 10-day repeat cycle. SLR/DORIS solutions are computed over 10-day arcs. GPS long arcs are "blended" together from the center 24 hours of 10 short arcs.

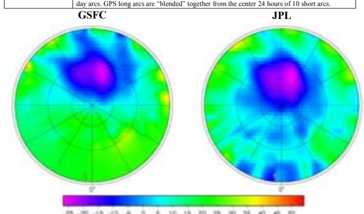

FIGURE 1 GPS antenna phase center maps (azimuth clockwise; 0º to 90º elevation from outside to center) The APC map estimated post-launch with GPS tracking data, is very important to POD. The 5ºx5º azimuth/elevation GSFC map was estimated in a formal solution using twelve 30-hr. arcs sampled over a β' cycle, and for which low elevation GPS double-difference phase data was edited. The JPL map (Haines et al., 2003b) was computed averaging one year of un-differenced GPS phase residuals into 5ºx2º azimuth/elevation bins.

Measurement Model Details: ***Proper modeling of the GPS antenna phase center is extremely important to the overall performance of the GPS based solutions. An antenna phase center map (APC map) has been developed both first at JPL (Haines et al. 2003) and then at GSFC (Luthcke et al. 2003) (Figure 1). Despite the fact these maps determined at the two centers were developed using very different solution techniques, data and editing, they show generally good agreement both capturing the same general features (Figure 1). Significant improvement in POD is obtained when using these maps (Table 3 and Figure 2). Additionally, to ensure precise modeling of the SLR observations, the LRA tracking point offset was adjusted in a formal least-squares solution using data from cycles 1-20. The new LRA offset improves the SLR model and the POD (Table 4).***

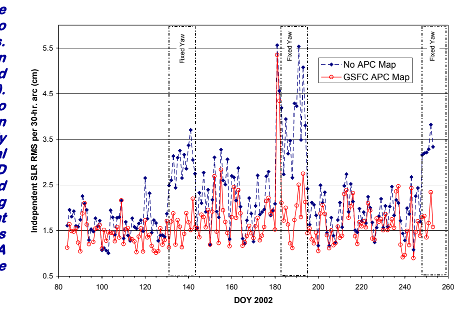

FIGURE 2 SLR residual test performance of GPS APC map.
Accurate modeling of the GPS antenna phase center is required for POD. The time series of independent SLR residuals RMS / 30-hour arc, cycles 8-24, show the benefit of using the GSFC APC map correction. This is especially evident over the fixed-yaw regime. The "No APC Map" phase center offsets had been adjusted from the pre-launch values and represent our best solution short of using the APC map.

Table 3 APC Map Performance in GPS RD Solutions: Residual Summary for Cycles 8-24

APC Map	GPS DDLC RMS (cm)	Independent SLR RMS (cm)	Independent Xover RMS (cm)
No APC Map	0.942	2.308	5.843
JPL APC Map	0.758	1.704	5.767
GSFC APC Map	0.752	1.701	5.766

Table 4 Summary of LRA Offset Analysis

Description	LRA offset spacecraft body-fixed coordinates (cm)			SLR residuals (cm) over cycles 1-20		SLR residuals (cm) over cycles 21-25 (independent data)	
	X	Y	Z	Mean	RMS	Mean	RMS
a-priori	117.1	59.8	68.28	-0.060	1.897	-0.214	1.799
estimated LRA offset	115.8	59.8	68.58	+0.049	1.835	-0.130	1.721
formal sigma	0.10	0.10	0.06				

POD Performance

Quantifying and Characterizing Orbit Error: ***Although the challenge of centimeter level POD is to quantify and characterize the orbit error, no direct measure of absolute orbit error exists. Therefore, we must use several different performance tests to help us gauge and understand the orbit error contained in the POD solutions. These orbit tests rely on the processing and analysis of all tracking data types available along with multiple solution techniques. In the analysis presented here we have investigated the POD performance using five candidate orbit solutions computed at GSFC. For a detailed comparison of the GSFC orbits to orbits computed at other centers see our poster: "Jason-1 POD Evaluation and Orbit Comparison", Zelensky et al.***

Tracking Data Residual Analysis: ***The results shown in Table 5 demonstrate the GPS-based reduced dynamic solutions represent a significant improvement over any orbit solution relying solely on SLR and DORIS tracking data. The GPS RD solution improvement in crossover RMS over SLR+DORIS Dyn represents 1.38 cm RMS in radial orbit accuracy improvement and 1.09 cm RMS radial orbit improvement over the SLR+DORIS RD solution. Adding SLR data to our GPS RD solution results in a further 0.4 cm RMS radial orbit improvement as indicated by the independent altimeter crossover residual statistics. The GPS-based orbits yield an excellent fit to the SLR data even though these data are withheld from the solutions. Furthermore, although the SLR data is not independent to the GPS+SLR RD solutions, we observe a stunning improvement in the SLR fits over any other solution that does not use GPS data indicating very good consistency between the GPS and SLR data. The results show the GPS-based solutions represent a significant improvement over SLR+DORIS Dyn. orbits considered to be accurate at the ~2cm radial RMS level. Further orbit improvement is obtained by using the GRACE derived GGM01S gravity model.***

The most direct measurement of radial orbit accuracy is obtained from high elevation SLR passes. Figure 3a shows the GPS RD solution independent high elevation SLR pass bias RMS for each station. It is important to note that while this is one of the most direct means for measuring radial orbit accuracy, it is not a perfect test and contains error sources other than radial orbit error (e.g. station position, LRA offset, and small component of horizontal orbit error). With this in mind the high elevation SLR analysis indicates the GPS RD orbit solutions have a radial orbit accuracy better than 1.25 cm.

Table 5 *Independent* and Dependent Data Residual Summary for Cycles 8-24

Solution Type	GPS DDLC RMS (cm)	DORIS RMS (mm/s)	SLR RMS (cm)	Xover RMS (cm)	Xover mean (cm)
Below with JGM3					
SLR+DORIS Dyn.		0.421	1.710	5.926	0.229
SLR+DORIS RD		0.418	1.665	5.867	0.219
SLR+DORIS+Xover RD		0.418	1.914	5.780	0.048
GPS RD	0.75	0.419	1.698	5.766	-0.026
GPS+SLR RD	0.77	0.419	1.341	5.750	-0.029
Below with GGM01S					
SLR+DORIS Dyn.		0.419	1.524	5.859	0.129
GPS RD	0.74	0.419	1.596	5.754	0.024
GPS+SLR RD	0.76	0.419	1.249	5.735	0.012

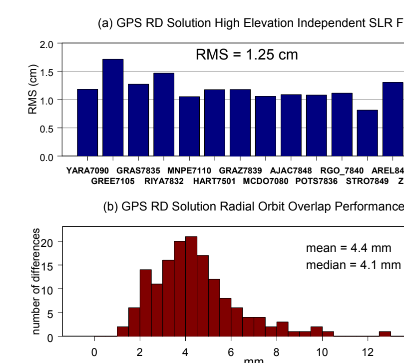

FIGURE 3 GPS RD (a) high elevation independent SLR fit and (b) radial orbit overlap performance.
(a) Measurement biases estimated from high elevation pass SLR residuals offer the best single metric to gauge radial orbit accuracy. The RMS of the estimated biases indicates orbit error does not exceed 1.3 cm. The actual radial error is less because the statistic contains other error sources as well. SLR data above 60 degrees are selected for the high elevation test. (b) Histogram of the radial orbit overlap difference RMS for each 6-hr. overlapping time period between GPS RD 30-hr. arcs from cycle 8-24. The result indicates the GPS reduced dynamic solutions are consistent to 4 mm.

Orbit Difference Analysis: ***Comparing orbits computed from independent tracking data can reveal systematic errors, especially measurement modeling errors. When comparing orbits computed from dynamic and reduced dynamic techniques, force modeling errors in the dynamic orbit and measurement modeling errors in the reduced dynamic orbit can be revealed (Christensen et al. 1994 and Marshall et al. 1995). A summary of our orbit difference analysis is presented in Table 6. The results show improved radial agreement is achieved by employing the reduced dynamic technique in the SLR+DORIS based solutions. Still further radial agreement is achieved by including altimeter crossover data in the SLR+DORIS RD solution. The results show it is possible to obtain 1-cm radial RMS orbit agreement between solutions computed from two independent sets of tracking data.***

Force modeling errors, such as mean geographically correlated gravity error and measurement modeling errors, such as realizations of the Terrestrial Reference Frame (TRF) can impart mean offsets in the ECF frame which can then adversely affect altimeter derived estimates of sea surface topography (Christensen et al. 1994 and Rosborough et al. 1986). For each cycle we have computed the mean orbit difference in the equatorial plane (RSS of the ECF X and Y mean) and in the Z direction. Table 6 shows the average and standard deviation of these statistics over cycles 8-24. The equatorial plane statistics show the reduced dynamic technique can be successfully applied in SLR+DORIS solutions to accommodate part of the known mean geographically correlated JGM3 gravity error. For the comparisons of the GPS RD solutions with SLR+DORIS based solutions (based on JGM3) the average of the mean Z ECF offset is less than 1 mm with standard deviation of less than 4 mm with a ~120-day periodicity (Figure 4). The dynamic SLR+DORIS solutions have traditionally served to monitor orbit consistency along the Z axis with an expected resolution of 5-6 mm. However, at the current level of agreement shown here it is not clear whether the SLR+DORIS or GPS-based orbits are dominating the remaining Z difference signal. Finally, we observe a ~4 mm mean Z offset between SLR+DORIS Dyn. and GPS RD solutions employing the GGM01S gravity model as compared to less than 1 mm observed using the JGM3 model. The results indicate the GGM01S gravity model imparts a mean Z offset that is better accommodated by the GPS RD solutions than the SLR+DORIS Dyn. solutions (Figure 4).

In addition to the statistics presented in Table 6, Figure 5 illustrates the improvements gained when employing the reduced dynamic technique in a SLR+DORIS based solution. Figure 6 illustrates the characteristics of the radial orbit differences between our GPS+SLR RD and SLR+DORIS Dyn solutions employing the GGM01S gravity model. Figure 6 illustrates the worst case errors expected in our best performing orbits (GPS+SLR RD) because the orbit difference is dominated by the errors in the SLR+DORIS Dyn. orbit. Nevertheless, the agreement between these orbits computed from different POD strategies and independent data is quite good.

Table 6 Orbit Difference Statistics Computed per Cycle and Summarized over Cycles 8-24

Solutions Differenced	Avg. Radial RMS (cm)	Avg. 3D RMS (cm)	Avg. / Stdev of RSS[mean XY] per cycle (cm)	Avg. / Stdev of mean Z per cycle (cm)
Below with JGM3				
GPS RD – SLR+DORIS Dyn	1.365	6.053	0.479 / 0.586	0.071 / 0.362
GPS RD – SLR+DORIS RD	1.141	4.809	0.376 / 0.437	0.069 / 0.380
GPS RD – SLR+DORIS+Xover RD	1.063	5.375	0.412 / 0.425	0.109 / 0.500
GPS RD – GPS+SLR RD	0.405	1.226	0.067 / 0.125	0.075 / 0.119
SLR+DORIS+Xover RD – SLR+DORIS Dyn.	0.946	5.396	0.591 / 0.271	-0.044 / 0.299
Below with GGM01S				
GPS RD – SLR+DORIS Dyn	1.178	5.015	0.144 / 0.570	0.422 / 0.327
GPS RD – GPS+SLR RD	0.370	1.122	0.089 / 0.113	0.131 / 0.112

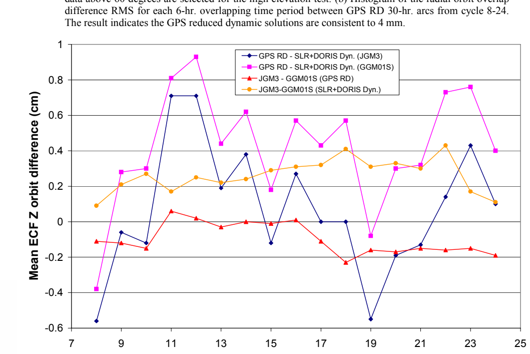

FIGURE 4. Mean ECF Z orbit difference per cycle.
The figure shows orbit consistency in the ECF *Z* axis between the GPS RD and SLR+DORIS Dyn. solutions. The dynamic SLR+DORIS orbit has traditionally served to monitor orbit consistency along the ECF *Z* axis with an expected resolution of 5-6 mm. The JGM3 based orbit differences demonstrate less than 1 mm mean and less than 4 mm standard deviation of the ECF Z per cycle mean orbit difference. Employing the GGM01S gravity model imparts a mean Z offset which is better accommodated in the GPS RD solutions.

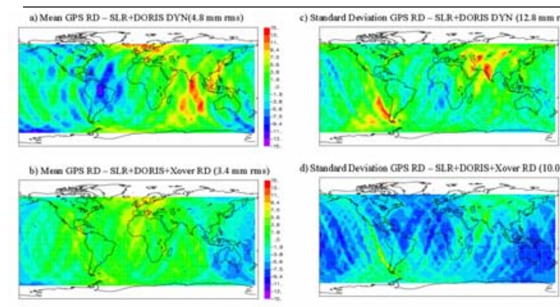

FIGURE 5 Radial orbit difference maps..
Radial orbit differences averaged over 5ºx5º bins for cycles 8-24, show that the geographically correlated JGM3 gravity error of about 5 mm observed in the SLR+DORIS dynamic solutions is significantly diminished in the SLR+DORIS+Xover reduced-dynamic orbit comparison (figures 5a, 5b). The figures show the geographically correlated JGM3 gravity error is significantly decreased when using the reduced dynamic technique even in a solution not computed from GPS data. The reduction in the standard deviation about the mean shown between the same two sets of orbit differences indicates the significant removal of geographically anti-correlated gravity error and possibly tide and nonconservative force modeling error when using the reduced-dynamic technique (figures 5c, 5d).

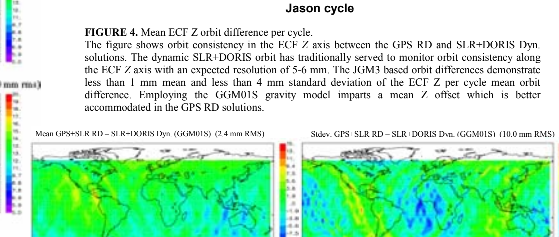

FIGURE 6 Radial orbit difference maps (GGM01S).
Radial orbit differences (GPS RD – SLR+DORIS Dyn.) averaged over 5ºx5º bins for cycles 8-24 using GGM01S. Comparison to Figure 5 shows significant reduction in geographically correlated and anti-correlated gravity error has been obtained using GGM01S. The differences are dominated by errors in the SLR+DORIS solutions and therefore illustrate the worst case errors expected in our best performing solutions (GPS+SLR RD).

Crossover Residual Analysis: ***Unlike orbit difference analysis, crossovers offer an important independent measure of orbit error such as the anti-correlated gravity error (Rosborough et al., 1986 and Scharoo and Visser, 1998). Figure 7 shows altimeter crossover residuals from cycles 8-24 averaged over 5ºX5º bins for three different types of orbit solutions. The three maps show a progressive and significant reduction of the radial orbit error from the SLR+DORIS Dyn, to the GPS+SLR RD solution to the GPS+SLR RD using the GGM01C gravity model. It should be noted that the crossover data contain non-orbit signal including altimeter measurement error and oceanographic signal. Therefore, caution should be exercised when interpreting these results as an absolute measure of radial orbit error. Nevertheless, this analysis can be used as a relative gauge of orbit error and clearly demonstrates the GPS RD solutions are accommodating a significant part of the JGM3 anti-correlated gravity error. Although the crossover variance is dominated by oceanographic signal and altimeter modeling error, we have also observed a significant reduction in crossover variance using the GPS-based RD solutions, as previously shown in Table 5.***

Figure 8 presents a time series of altimeter crossover means computed globally per cycle. The SLR+DORIS Dyn solutions show a larger variation and mean than the GPS-based RD orbits (also see Table 5). Of particular interest in Figure 8, is the 60-day signature in the mean altimeter crossover residual time series clearly observed by the GPS-based orbit solutions. Orbit solutions based on SLR+DORIS data also see this 60-day signature but are much noisier or have an additional signal superimposed. The data in Figure 8 also show that employing a reduced dynamic technique or the GGM01S gravity model does not significantly change this signal lending input to the notion that this signal is not likely a force modeling error. Furthermore, because this signal is observed in both SLR+DORIS and GPS-based solutions and because of its 60-day periodicity it is not likely due to mean offsets of the orbit in the inertial frame. This signal may be due to a non-orbit effect such as mis-modeling of surface tides, ionosphere or atmospheric pressure corrections. This analysis demonstrates that the significant improvement in orbit accuracy achieved with the GPS(+SLR)-based RD solutions will enable the resolution of new signals and features within the altimetry.

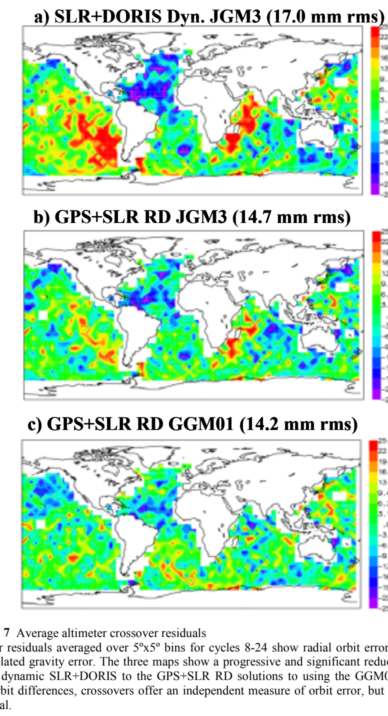

FIGURE 7 Average altimeter crossover residuals
Crossover residuals averaged over 5ºx5º bins for cycles 8-24 show radial orbit error primarily due to anti-correlated gravity error. The three maps show a progressive and significant reduction of this error from the dynamic SLR+DORIS to the GPS+SLR RD solutions to using the GGM01 gravity model. Unlike orbit differences, crossovers offer an independent measure of orbit error, but also contain non-orbit signal.

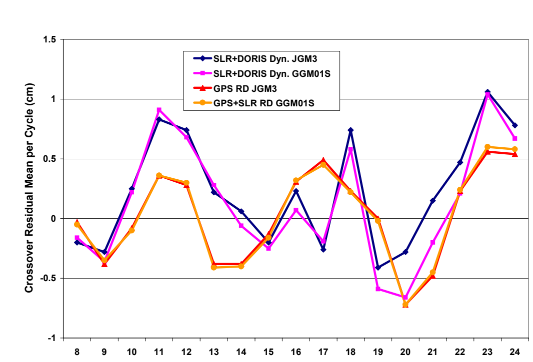

FIGURE 8 Crossover residual mean time series.
Altimeter crossover residual means, cycles 8-24, show that the least variation and mean are observed using the GPS-based orbits. The interesting, approximately 60-day signature, observed using all of the orbits and best seen with the GPS-based orbits, may be due to a non-orbit effect such as mis-modeling of surface tides, ionosphere or atmospheric pressure corrections.

References:

Christensen, E.J., B.J. Haines and K.C. McColl, "Observations of geographically correlated orbit errors for TOPEX/Poseidon using the global positioning system," *Geophysical Research Letters*. 21(19): 2175-2178, 1994.

Haines, B., W. Bertiger, S. Desai, D. Kuang, T. Munson, L. Young and P. Willis, "Initial Orbit Determination Results for Jason-1: Towards a 1-cm Orbit," Journal of Navigation, in press, 2003.

Luthcke, S.B., N.P. Zelensky, D.D. Rowlands, F.G. Lemoine and T.A. Williams, "The 1-centimeter Orbit: Jason-1 Precision Orbit Determination Using GPS, SLR, DORIS and Altimeter data," *Marine Geodesy*, Special Issue on Jason-1 Calibration/Validation, Part 1, Vol. 26, No. 3-4, 2003.

Marshall, J.A., N.P. Zelensky, S.B. Luthcke, K.E. Rachlin, and R.G. Williamson, "The Temporal and Spatial Characteristics of TOPEX/Poseidon Radial Orbit Error," *Journal of Geophysical Research*. 100(c12): 25,331-25,352, 1995.

Rosborough, G. W., "Satellite orbit perturbations due to the Geopotential," Ph.D. dissertation, Center for Space Research, The University of Texas at Austin, 1986.

Scharroo, R., and P.N.A.M Visser, "Precise orbit determination and gravity field improvement for the ERS satellites," *Journal of Geophysical Research*, 103: 8113-8127, 1998.

Contact Information:
Scott B. Luthcke
NASA Goddard Space Flight Center
Space Geodesy Branch, Code 926
Phone: (301) 614-6112
email: Scott.B.Luthcke@nasa.gov

Acknowledgements:

We wish to thank Bruce Haines for the JPL GPS APC map, several RINEX data sets, and discussions pertaining to the Jason-1 BlackJack GPS receiver. We also wish to thank Jean Paul Berthias and the CNES POD team for the prelaunch satellite characteristic definitions and models and for distribution and assistance with supporting Jason-1 data. We also acknowledge the NASA physical oceanography program and the TOPEX/Poseidon project for their support.

Presented at:
Jason-1 and TOPEX/Poseidon SWT meeting
Aries, France, Nov. 17th-21st, 2003